ELSEVIER

Journal of Chromatography A, 794 (1998) 15–25

JOURNAL OF CHROMATOGRAPHY A

Application of liquid chromatography–mass spectrometry^n analyses to the characterization of novel glyburide metabolites formed in vitro

P.R. Tiller[a,*], A.P. Land[a], I. Jardine[a], D.M. Murphy[b], R. Sozio[b], A. Ayrton[b], W.H. Schaefer[b]

[a]*Finnigan MAT, 355 River Oaks Parkway, San Jose, CA 95134, USA*
[b]*SmithKline Beecham Pharmaceuticals, 709 Swedeland Road, King of Prussia, PA 19406, USA*

Abstract

The application of bench-top ion-trap atmospheric pressure ionization mass spectrometry in the characterization of in vitro metabolites of glyburide is discussed. The metabolites formed in vitro by rat, dog, monkey and human liver microsomes were separated by reversed-phase high-performance liquid chromatography (HPLC) and characterized by mass spectrometry $(MS)^n$ experiments. The utility of data dependent MS1–MS2–MS3 analyses, where the mass spectrometer makes ''real-time'' decisions about the experiment to be performed, are described using the characterization of two novel metabolites of glyburide as an example. The metabolite profiles from each species were similar. Six cyclohexyl hydroxylation products were detected, as well as two novel monooxygenation products formed via hydroxylation of the ethyl chain at the benzylic position, and alpha to the amide nitrogen. The ion-trap with electrospray ionization proved to be a sensitive and reliable HPLC detection system that provided important chemical structure information. © 1998 Elsevier Science B.V.

Keywords: Mass spectrometry; Pharmaceutical analysis; Glyburide; Sulfonylureas

1. Introduction

Metabolism studies using both in vitro and in vivo methods are key to the characterization of new drug candidates. The goals of these studies include determination of the routes by which the molecules are metabolized, how rapidly they are metabolized and characterization of the metabolites that are formed. Typically, the metabolic profiles from several different species are determined to compare the metabolism of a compound in the animal species used for toxicology testing to that in humans.

The advent of atmospheric pressure ionization (API) sources [including electrospray (ESI) and atmospheric pressure chemical ionization (APCI)] has revolutionized the analysis of drug and metabolites in biological samples. With their ease of coupling directly with high-performance liquid chromatography (HPLC), high sensitivity, suitability for a wide range of analytes, including polar involatile (biological) molecules, API sources are an ideal interface to mass spectrometry (MS). Currently, much of this work is carried out using triple quadrupole mass spectrometers as MS–MS is an essential element in such studies. Typically, several LC–MS and LC–MS–MS analyses are required to locate sites of metabolism using an iterative process, where the information from one experiment is used to

*Corresponding author.

0021-9673/98/$19.00
PII S0021-9673(97)00881-9

define the subsequent analysis. Thus, many experiments may be required on each sample to obtain sufficient data to characterize all of the metabolites. Still, the data obtained using a triple quadrupole instrument may not be sufficient to distinguish between several possible structural isomers.

Modern ion-trap technology [1,2] with MS^n capability has the potential to define the sites of metabolism more clearly. The current API ion-trap mass spectrometers, in addition to generating MS^n data, are able to conduct automated data-dependent analyses, yielding valuable information ''on-the-fly''. This means that the mass spectrometer will select MS^n experiments based on the data from previous scans, thus performing the multi-experiment analysis, necessary using a triple quadrupole, in one experiment. An example of the application of data-dependent MS^n analyses using an ion-trap mass spectrometer, to metabolite characterization is described for glyburide metabolites formed in vitro.

Glyburide (glibenclamide) is a potent sulfonylurea drug which has been used widely in the treatment of non-insulin-dependent *diabetes mellitus* for more than 25 years [3,4]. The metabolism of glyburide has been described in animals [5] and man [6], and it was found to be metabolized extensively via oxidative pathways. Glyburide is commonly studied in drug interaction studies with new drug candidates; however, the enzymes that catalyze the biotransformation of glyburide have not, as yet, been described. We have used HPLC coupled to a modern ion-trap MS with ESI to investigate the biotransformation of glyburide in vitro to begin to facilitate characterization of the enzymology of these reactions.

2. Experimental

2.1. Reagents

Acetonitrile was obtained from Burdick and Jackson (WI, USA). NADP, glucose-6-phosphate and glucose-6-phosphate dehydrogenase were obtained from Sigma (St. Louis, MO, USA). HPLC-grade water was obtained from a Milli-Q system (Millipore, Milford, MA, USA).

2.2. Microsomal incubations

Microsomal fractions were prepared from rat, dog and human liver as described previously [7]. Reaction mixtures (250 μl) containing 5 or 50 μ*M* glyburide, 1 mg of microsomal protein/ml, 0.1 *M* potassium phosphate pH 7.25, 1 m*M* NADP, 10 m*M* glucose-6-phosphate and 1 unit of glucose-6-phosphate dehydrogenase/ml were incubated at 37°C for 30 min. The reactions were quenched by addition of 250 μl of acetonitrile and the precipitated material was removed by centrifugation. The supernatant was diluted with 500 μl of 10 m*M* ammonium acetate pH 5.0 prior to analysis by LC–MS to reduce the acetonitrile concentration and preserve chromatographic peak shape.

2.3. LC–MS^n of glyburide metabolites

Nearly all of the LC–MS and LC–MS^n analyses were done using the 5 μ*M* incubation samples. Some of the negative ion analyses were conducted using the 50 μ*M* samples. Metabolic products were separated using Hitachi L-7100 ternary HPLC pumps (Hitachi Instruments, San Jose, CA, USA) with a CTC A200F autosampler (Leap Technologies, Chapel Hill, NC, USA) using a Prodigy, 5 μm, C_8, 150×2 mm column with a 10×2 mm guard column (Phenomenex, CA, USA). Solvent A was 10 m*M* ammonium acetate pH 5.0 and solvent B was acetonitrile. The compounds were eluted using the following linear gradient: 0 min, 30% B; 15 min, 30% B; 30 min, 100% B; 35 min, 100% B; 36 min, 30% B; 46 min, 30% B; flow 0.2 ml/min. The entire 0.2 ml/min flow was directed into the source of the LCQ API mass spectrometer (Finnigan, San Jose, CA, USA) without splitting, with the first 2.1 min diverted to waste using the built-in automated divert valve. The heated capillary was operated at 250°C and sheath and auxiliary gases were set to 80 and 25, respectively. The instrument was set to acquire 3 microscans with a maximum trap injection time of 200 ms/microscan. A relative collision energy of 25% was used for all MS^n experiments with an isolation width of 7.0 u to allow collection of both ^{35}Cl and ^{37}Cl isotope peaks within a single scan. The 7.0 u isolation window resulted in collection of ions (3.5 u from the parent set mass. Thus, with data-

dependent analyses, the instrument automatically selected the $[M+H]^+$ for the ion of interest (containing ^{35}Cl) at the center of the isolation window and the wide window facilitated isolation of the ^{37}Cl-containing ion also. Although an isolation width of 7.0 u was used to collect ions for MS^n experiments, the product ions were analyzed at unit resolution. With ion-trap technology, the collection (or trapping) of ions is distinct from the ejection (or analysis) of ions, so the 7.0 u isolation width did not result in decreased resolution of the analysis [12]. In some experiments an isolation width of 1.2 u was selected to acquire spectra for monoisotopic ions.

3. Results

3.1. Strategy

Each of the microsomal incubation samples were analyzed by LC–MS and LC–MS^n to determine the profiles of metabolites formed, as well as to characterize the metabolite structures. Data-dependent analyses facilitated acquisition of the majority of these data from a single HPLC analysis. Profiles of the metabolites formed were described by reconstructed ion chromatograms from full scan MS1 experiments. Structural information was provided by MS2 and MS3 experiments conducted automatically during the analysis. The metabolites characterized in these experiments were formed using liver microsomal fractions fortified with nicotinamide adenine dinucleotide phosphate (NADPH). Thus, only oxidation reactions were supported. Possible oxidation products for glyburide included monooxygenation (+16 u), dioxygenation (+32), and monooxygenation to form a hydroxyl with subsequent oxidation to a carbonyl (+14), oxidative demethylation, and combinations of multiple oxidation reactions. A list of ions corresponding to the $[M+H]^+$ for glyburide and its potential metabolites was entered in the method setup for the analysis in order to prevent the instrument from obtaining spectra on irrelevant, but potentially intense, ions in the samples. When one of the ions from the list was detected in the MS1 scan and passed above a threshold, the mass spectrometer automatically acquired a product ion mass spectrum (MS2) for this ion. If more than one ion from the list are coeluting, the most intense ion is selected. (Therefore, the MS1 data should be evaluated carefully to determine whether coeluting components are present, and subsequent experiments would have to be conducted to acquire MSn data on these less abundant products.) Next a product ion MS3 mass spectrum was also collected for the base peak from the MS2 spectrum. This MS1–MS2–MS3 sequence was repeated throughout the duration of the chromatographic peak. At the end of the peak, the mass spectrometer returned to MS1 mode until another ion from the mass list was detected and the cycle was repeated for this new ion. This single analysis provided a metabolite profile, molecular masses for the metabolites and structural information. Additional structural data were collected from subsequent LC–MS^n analyses designed to collect MS2 and MS3 data for specific ions of interest.

In the case of samples where the species of interest are entirely unknown, the approach would be to have the instrument automatically select the most intense ion in the spectrum that passes above a threshold set by the operator. The rest of the multistage MS^n experiment would be identical to that described above.

3.2. Metabolite profiles

The metabolite profiles shown in Fig. 1 for each species examined were qualitatively very similar. The only metabolites formed in significant quantities in these reactions were those resulting from monooxygenation (+16 u at m/z 510). Fig. 1, panel A displays the reconstructed ion current (RIC) for unchanged glyburide (m/z 494, 26.1 min) that remained in the rat microsomal sample at the end of the incubation. Panels B, C, D and E show the RICs for detected glyburide metabolites (m/z 510) formed with rat, dog, monkey and human liver microsomes, respectively. Based on relative peak heights, approximately 5–50% of the glyburide was converted to metabolites in the 5 μM incubations and approximately 5–20% in the 50 μM incubations for each species. The relative amounts of each of the metabolites formed with the 5 and 50 μM incubations were similar. A group of metabolites that eluted early in the chromatogram (8.7–16.9 min) were separated during an isocratic period in the chromatographic

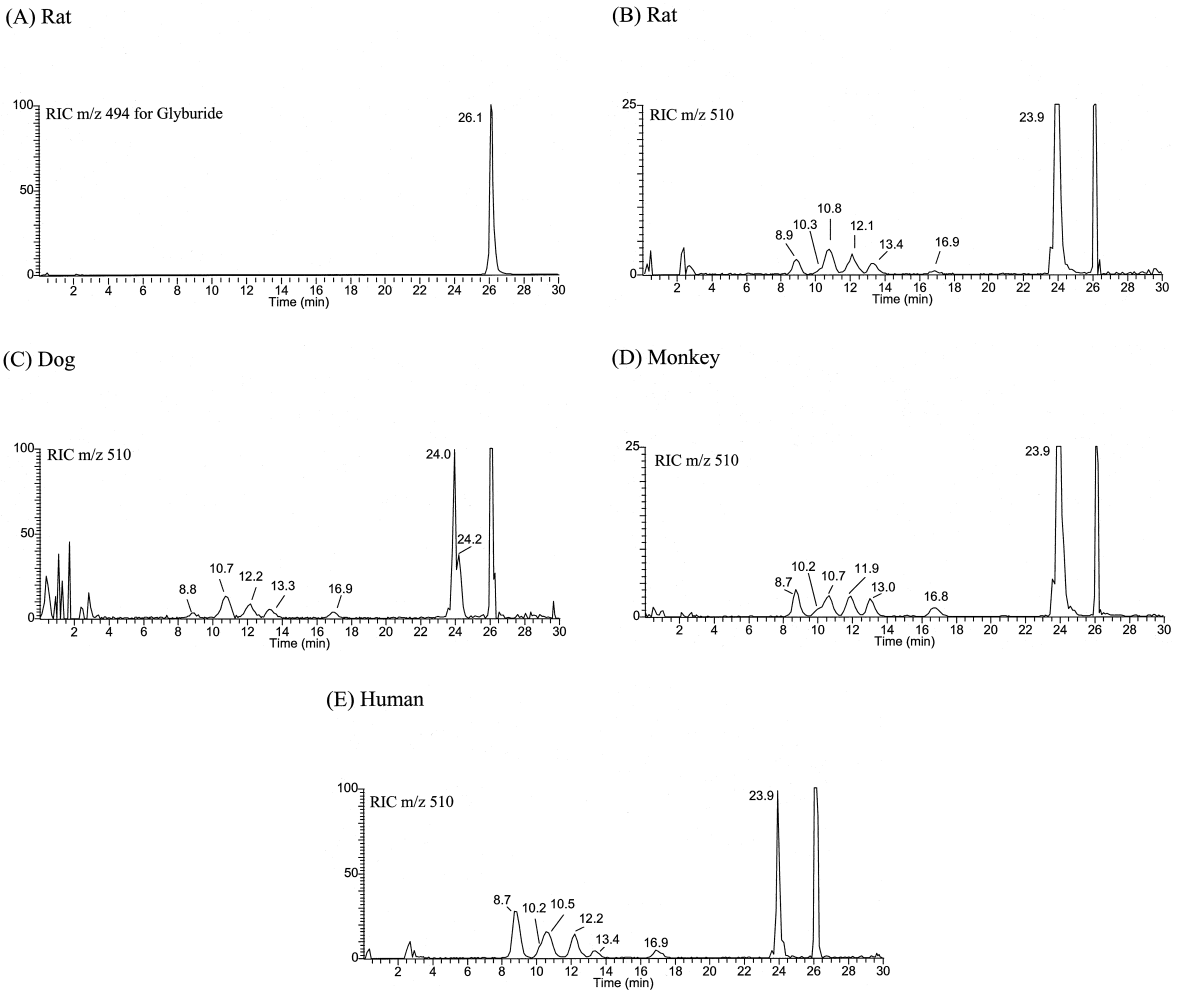

Fig. 1. RICs for unchanged glyburide (m/z 494) in a rat microsomal sample (A) and for metabolites (m/z 510) in rat (B), dog (C), monkey (D) and human (E) liver microsomal samples.

method. These products showed addition of 16 u relative to glyburide and were observed with rat, dog and human liver microsomes. Two novel, closely eluting metabolites at 23.9 and 24.2 min also displayed addition of 16 u. The metabolite at 23.9 min was observed in all species tested, but the metabolite at 24.2 min was only detected in dog and some human liver microsomal samples. The relative amounts of the early eluting metabolites compared to the two later eluting metabolites varied quite dramatically between microsomes from five different human liver samples studied. In some human samples, the 23.9 min metabolite was predominant, while in others the 8.7 min peak was most abundant (data not shown). The metabolites that eluted between 8.7–16.9 min were readily detected in all human samples. The 23.9 min metabolite was significant in most human samples except in two where it was present in trace amounts. The peak at m/z 510 that coeluted with unchanged glyburide appeared to correspond to the cluster of ions associated with an ammonium adduct of glyburide. The intensity of this peak was small relative to that at m/z 494 for glyburide.

3.3. Glyburide

Glyburide was characterized using MS2, MS3 and MS4 experiments during infusion of a 1 μg/ml stock solution and the spectra are shown in Fig. 2. These spectra were used as references to aid in interpretation of the spectra for metabolites. Shifts in masses observed for metabolites relative to spectra for glyburide, as well as differing fragmentation patterns facilitated characterization of the metabolite struc-

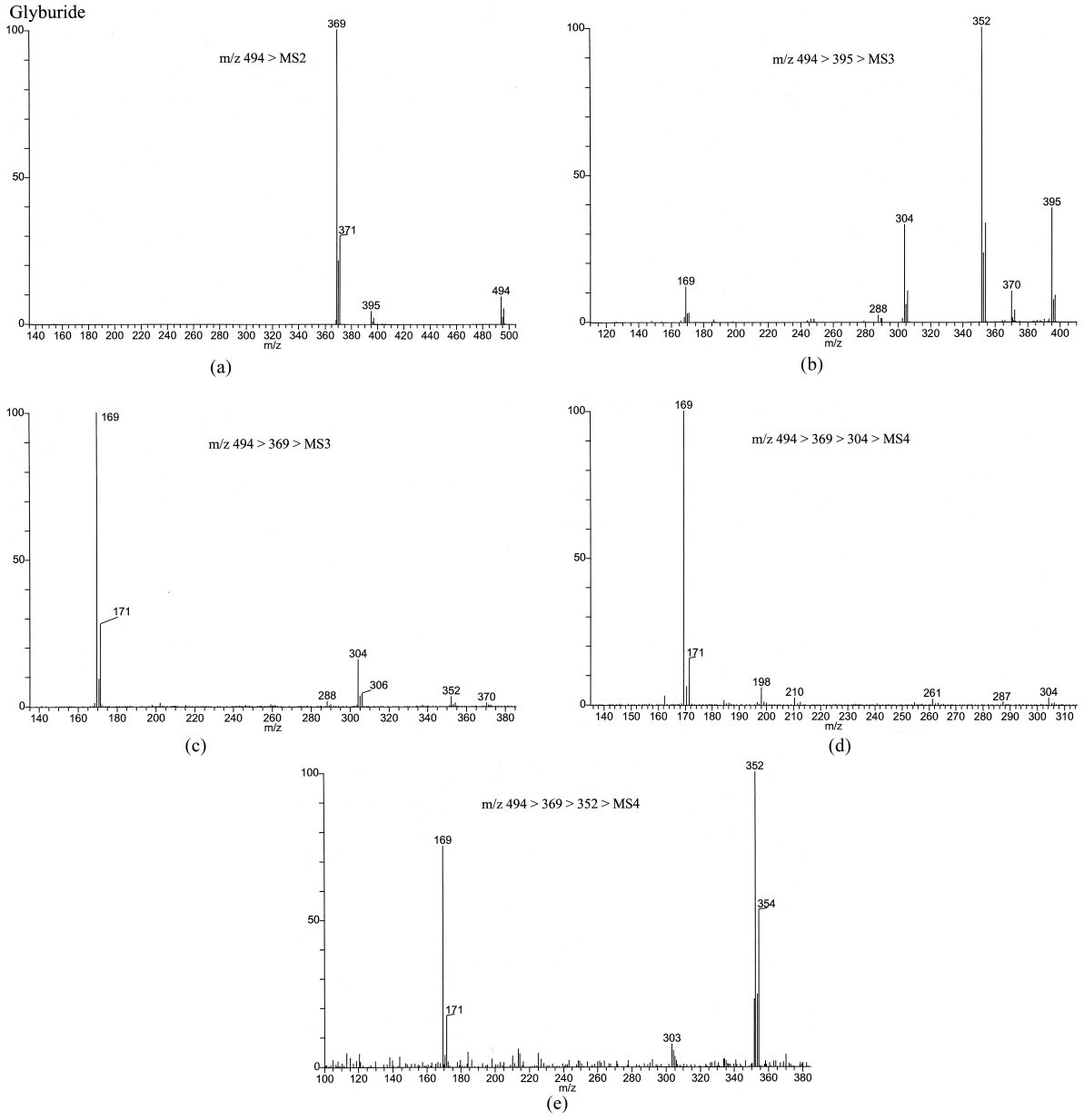

Fig. 2. MS^n spectra for glyburide.

tures. A 7 u wide window was used to collect the precursor ion for product ion experiments in order to capture both ^{35}Cl- and ^{37}Cl-containing ions. Thus, the product ions also showed the presence or absence of a Cl isotope pattern that was diagnostic for proposing structures for the ions. The product ion spectra collected in an MS2 experiment for the $[M+H]^+$ at m/z 494 yielded a relatively simple spectrum with ions at m/z 395 and 369 that corresponded to elimination of cyclohexylamine and cyclohexylisocyanate, respectively, as shown in Fig. 3. Further fragmentation of the ion at m/z 395 in an MS3 experiment produced ions at m/z 370, 352, 304 and 169. The ion at m/z 370 appeared to be an H_2O adduct of the ion at m/z 352 formed in the ion-trap [8,9]. Note that the m/z 395 ion could not dissociate to form the ion at m/z 369 because it lacked a sufficient number of protons. An MS3 experiment selecting the ion at m/z 369 yielded ions at m/z 370, 352, 304, 288 and 169. In an MS4 experiment, the ion at m/z 304 produced ions at m/z 210, 198 and 169. Further fragmentation (MS4) of the ion at m/z 352 yielded the m/z 169 ion. Each of the ions observed contained a characteristic Cl isotope pattern. Glyburide also formed a reasonably intense $[M-H]^-$ under negative ion conditions. An MS2 experiment using the $[M-H]^-$ at m/z 492 yielded ions at m/z 460, 378, 367, and 170. The ion at m/z 460 corresponded to an unusual loss of 32 u (either CH_3OH or O_2) from the $[M-H]^-$ at m/z 492 and the ion at m/z 367 was formed by elimination of cyclohexylisocyanate. Further dissociation of the ion at m/z 460 produced ions at m/z 378 (elimination of cyclohexene, 82 u) and 170. Dissociation of the ion at m/z 367 produced only the ion at m/z 170. In each case the ion at m/z 170 was found to contain the chlorine atom, but the structure of the ion was ambiguous. Although the negative ion MS2 spectrum for glyburide showed ions at m/z 460 and 378, the MS3 spectrum of the m/z 460 ion also produced the ion at m/z 378. This data indicated that the m/z 378 ion resulted from loss of the 32 u moiety and cyclohexene, and confirmed the structural relationship between these ions.

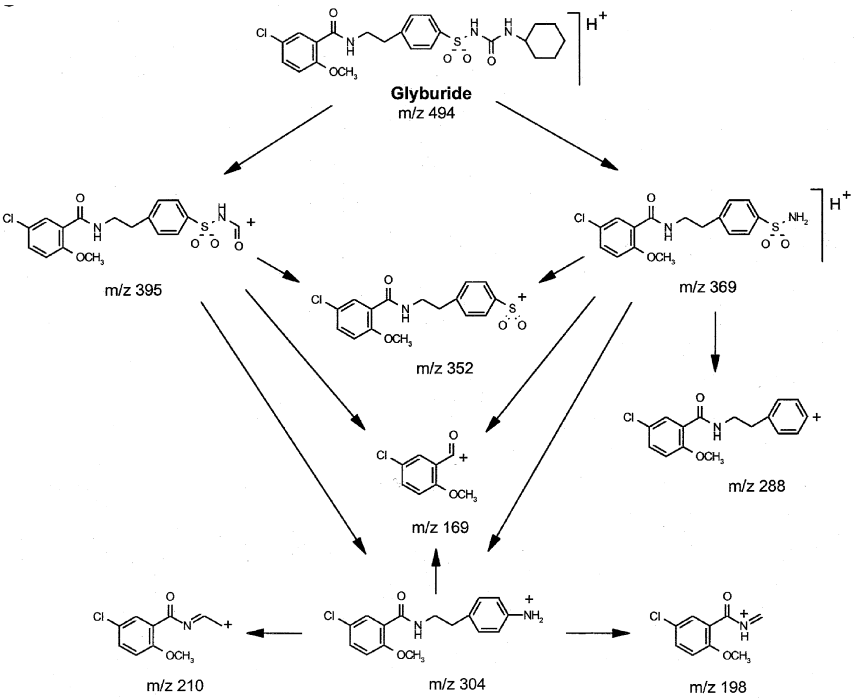

Fig. 3. Proposed fragmentation scheme for glyburide.

3.4. 8.7–16.9 min peaks

Glyburide contains seven potential sites for hydroxylation on the cyclohexyl ring (since the axial and equatorial positions are not equivalent). Product ion mass spectra indicated that the first group of approximately six metabolites that eluted between 8.7 (see Fig. 4) and 16.9 min were all hydroxylated on the cyclohexyl ring. A small shoulder preceding the 12.1 min peak that was evident in MS2 analyses represented a 7th metabolite in some samples. Each displayed an $[M+H]^+$ at m/z 510. Structural characterization of these metabolites using the automated data dependent analysis procedure described above provided intense spectra with readily apparent chlorine isotope patterns on each of the product ions. Each of these metabolites showed very similar product ion mass spectra characterized by elimination of H_2O (m/z 492) from the $[M+H]^+$ and formation of the ions at m/z 395 and 369 from elimination of hydroxycyclohexylamine and hydroxycyclohexylisocyanate. Although each of the metabolites displayed elimination of H_2O (m/z 492), the metabolite that eluted at approximately 13.4 min and the small shoulder that preceded the 12.1 min peak both showed m/z 492 as the base peak in the MS2 spectra. The ion at m/z 369 was the base peak for the other metabolites. MS3 analyses of the ion at m/z 492 produced ions at m/z 395, 369, 304 and 169, the same as those produced from glyburide, and confirmed the cyclohexyl as the site of oxygenation. Further dissociation of the ion at m/z 369 also yielded the same spectrum that was observed for glyburide.

3.5. 23.9 and 24.2 min peaks

An additional pair of metabolites, not previously

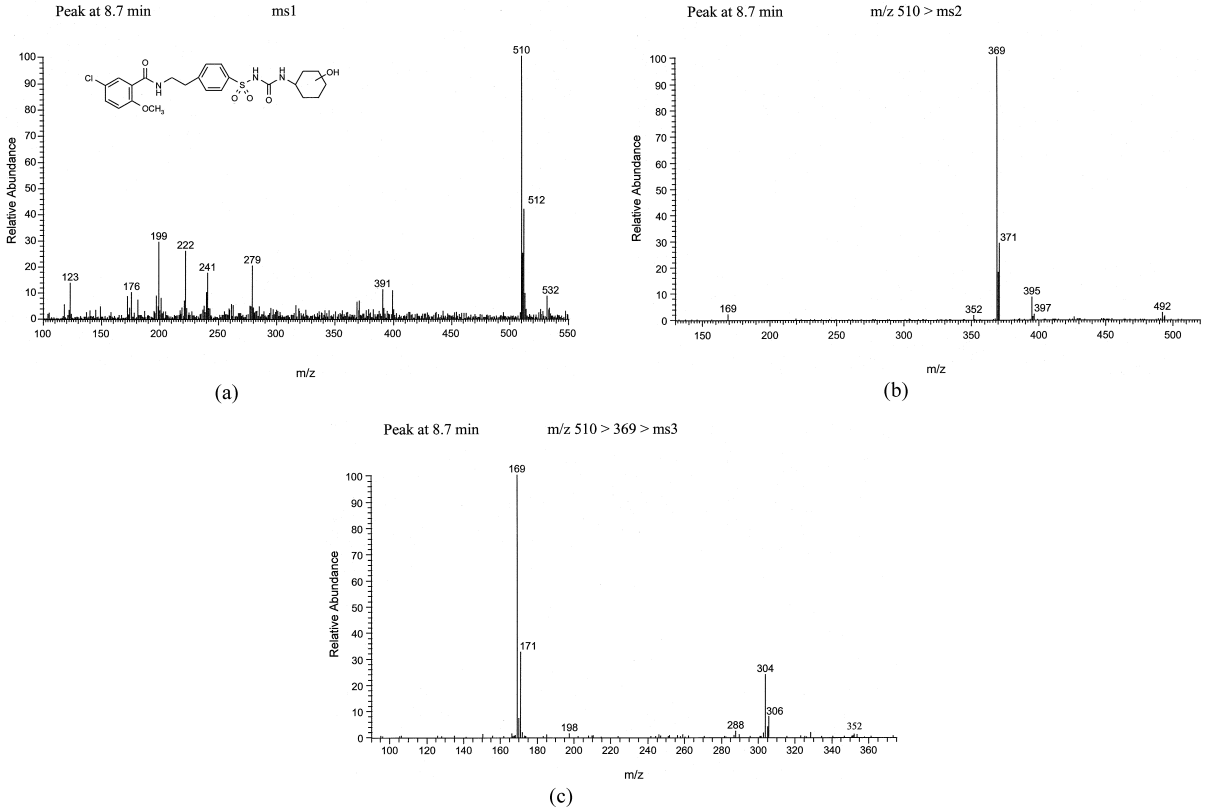

Fig. 4. MS^n spectra for the metabolite at 8.7 min.

reported, also showed monooxygenation (+16), but eluted later than the hydroxycyclohexyl metabolites. The two later eluting metabolites at 23.9 and 24.2 min displayed an $[M+H]^+$ at m/z 510, but showed rather different mass spectral characteristics. The MS2 spectrum of the 23.9 min metabolite produced ions at m/z 411 (elimination of cyclohexylamine), 385 (elimination of cyclohexylisocyanate) and 367 (elimination of cyclohexylisocyanate and H_2O), and a very small signal at m/z 492 (elimination of H_2O). Further dissociation of the ion at m/z 411 resulted in elimination of H2O and formation of an ion at m/z 169 (2-chloro-6-methoxybenzoxy) and dissociation of the m/z 385 ion resulted in loss of H_2O and NH_3 (m/z 350), and formation of the m/z 169 ion (Figs. 5 and 6). The ions at m/z 411 and 385 indicated that hydroxylation did not occur on the cyclohexyl ring. The ions at m/z 492 and 367 corresponded to elimination of H_2O indicating that hydroxylation had not occurred on an aromatic ring. The structures in Fig. 6 that showed elimination of water were consistent with oxygenation on the ethyl group, but oxygenation to form a hydroxamic acid could not be ruled out based on the mass spectra alone. Dissociation of the ions at m/z 510, 385 and 367 yielded an ion at m/z 169 that corresponded to a 2-chloro-6-methoxybenzoxy ion and confirmed that the chlorophenyl ring had not been hydroxylated. Thus, the ethyl amide bridge was the site of hydroxylation, although the exact position could not be determined from the positive ion mass spectra. [Preliminary NMR spectra for the 23.9 min peak were consistent with hydroxylation at the benzylic position (data not shown)].

The product ion mass spectrum for the 24.2 min peak (m/z 510) was similar to that for the 23.9 min peak (data not shown). The ions at m/z 411, 385 and 367 were present at similar relative abundances to those for the 23.9 min peak, but the ion at m/z 492 was the base peak in the spectrum for the 24.2 min peak. Further dissociation of the m/z 492 ion yielded ions at m/z 410 (elimination of cyclohexene), 393

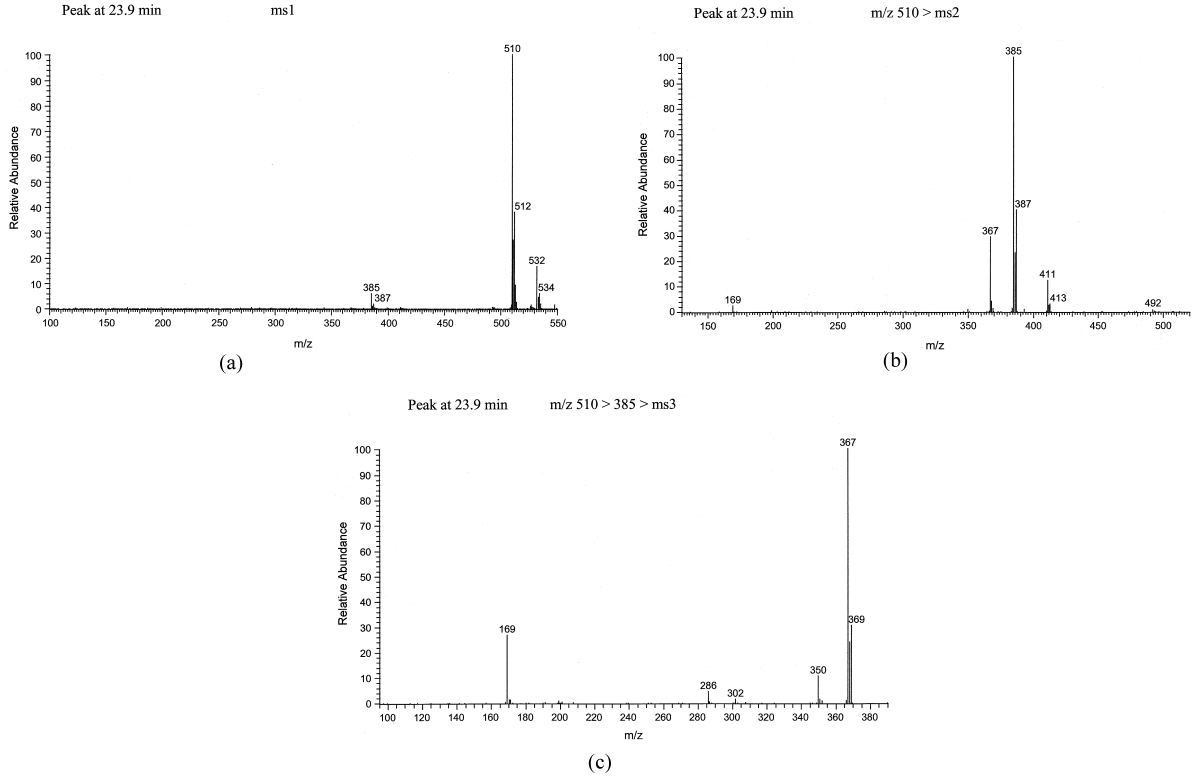

Fig. 5. MS^n spectra for the metabolite at 23.9 min.

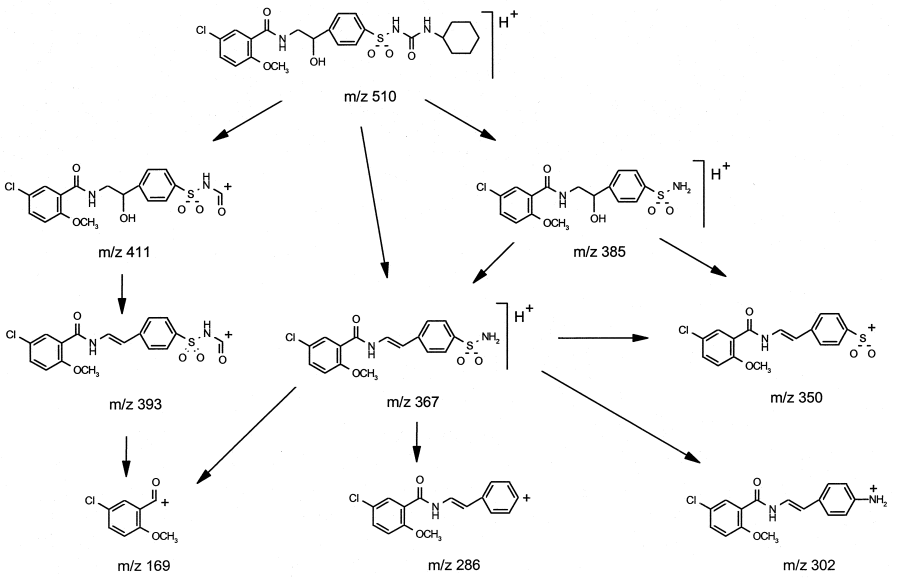

Fig. 6. Proposed fragmentation scheme (positive ion) for ethylhydroxy metabolite of glyburide that eluted at 23.9 min.

(elimination of cyclohexylamine), 367 (elimination of cyclohexylisocyanate), 350 (elimination of cyclohexylurea) and 169. Similar to the 23.9 min peak, these ions indicated addition of oxygen to the ethylamide portion of the molecule, but did not reveal the exact position.

Negative ion spectra (data not shown) were also obtained for these metabolites to provide additional structural information. The product ion spectra in negative ion mode showed striking differences for the 23.9 and 24.2 min peaks. The product ion spectrum for the $[M-H]^-$ at m/z 508 of the 23.9 min peak was very similar to that observed for glyburide, except most of the ions were shifted by 16 u (m/z 476, 394, 383) consistent with the addition of an oxygen atom. The spectrum for the 23.9 min peak did not provide any additional structural information over that obtained from the positive ion spectra. However the product ion spectrum for the $[M-H]^-$ at m/z 508 of the 24.2 min peak displayed a base peak at m/z 323 that was not observed with the 23.9 min peak, in addition to ions at m/z 476, 394, and 383 (summarized in Fig. 7). The ion at m/z 323 corresponded to elimination of 2-chloro-6-methoxybenzamide from the metabolite with retention of the oxygen atom on the charged fragment. Further dissociation of this ion yielded ions at m/z 198 and 134 that were consistent with retention of the oxygen following elimination of cyclohexylformamide and an additional expulsion of SO_2, respectively. Thus, the position of the oxygen atom significantly effected the fragmentation of this metabolite in negative ion mode. The ion at m/z 323 in the negative ion spectra and the facile elimination of H_2O in the positive ion spectra were consistent with oxygenation of the ethyl

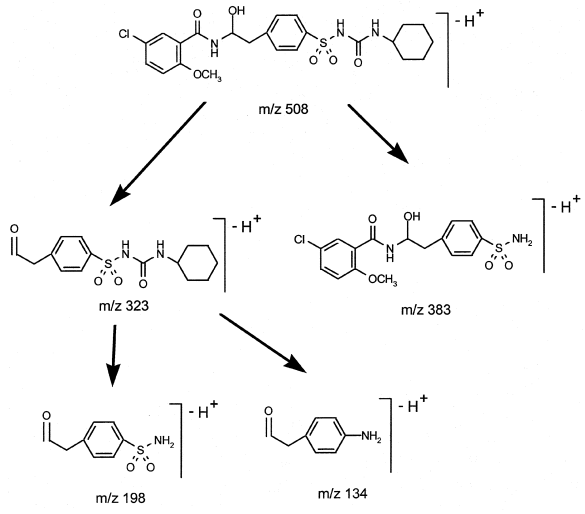

Fig. 7. Proposed fragmentation scheme (negative ion) for the ethylhydroxy glyburide metabolite that eluted at 24.2 min.

side chain. Cleavage adjacent to the amide would be increased with presence of a hydroxyl on the carbon linked to the amide nitrogen. Although this structure may be expected to be relatively unstable, a metabolite of the vasopressin V1 receptor antagonist OPC-21268 with a similar structure was isolated from dog, rat and human urine and confirmed by synthesis [10,11]. Thus, two metabolites were identified that were hydroxylated on the ethyl chain. The metabolite that eluted 24.2 min was assigned with hydroxylation at the methylene adjacent to the amide nitrogen and the 23.9 min peak was hydroxylated at the benzylic position.

4. Discussion

The biotransformation of glyburide has been described previously for dog, rat, rabbit and human [5,6]. The metabolites observed using rat, dog and human liver microsomes were consistent with those reported in vivo, although several new metabolites were observed in vitro. The predominant metabolites in vivo in each species were the 4-*trans*-hydroxycyclohexyl and 3-*cis*-hydroxycyclohexyl products. Cyclohexyl hydroxylation products were also formed with liver microsomes from rat, dog and human, but at least six cyclohexyl hydroxylation products were observed in vitro. In vivo experiments with rat, dog and rabbit showed formation of 3-chloro-6-methoxybenzamide that would likely arise from hydroxylation adjacent to the amide nitrogen with subsequent elimination. An ethylene metabolite was also identified in vivo that could have been formed by hydroxylation on the ethyl bridge with subsequent elimination of H_2O (possibly during sample processing). A benzoic acid product observed in vivo in rat could also have arisen from oxidation of the ethyl bridge with subsequent cleavage and oxidations to yield a carboxylic acid. Consistent with these in vivo metabolites, the microsomal incubations showed production of two metabolites that were formed via addition of oxygen to the ethylamide portion of glyburide. These ethylamide oxidation products were not described previously in the in vivo studies.

The microsomal incubations with glyburide yielded a complex mixture of metabolites. Characterization of these metabolites using the ion-trap proved to be a sensitive and convenient approach. The capability of acquiring data using automated data dependent analyses allowed a broad range of data, including molecular mass, retention time and structure information, to be collected from a single LC–MS run. Although MS2 experiments provided valuable structure information, further MS3 and MS4 experiments provided additional structural information, and helped fragmentation pathways and fragment ion structures to be assigned more confidently by elucidating the sequence of fragmentation reactions, as well as revealing structural features of the precursor ions. In addition, the ability to select a wide window for parent ion peaks for MS^n experiments without loss of sensitivity or resolution allowed isotope ratios (such as that for chlorine) to be visible from a product ion experiments further aiding in interpretation of spectra. Although the MS^n analyses clearly indicated the regions where hydroxylation occurred, nuclear magnetic resonance (NMR) analyses are required to prove the exact positions of hydroxylation, especially for the cyclohexyl hydroxylation products.

Automated data-dependent LC–MS^n is a screening experiment that is generic in its application [13–16]. It is currently being used to identify mixtures of unknowns in natural products discovery applications, in metabolite identification, drug impurity analysis and formulation degredent studies. The last three applications share a common analytical motif in that they involve a single known compound, the original drug and a series of unknowns, the metabolites, impurities or degredents. Therefore, the experimental protocol discussed in this paper has application in many aspects of both drug discovery and drug development.

5. Conclusions

The API ion-trap mass spectrometer interfaced to an HPLC has proven to be a sensitive, convenient, economical and reliable instrument for characterizing structures of metabolites in biological samples. The automated features allow valuable structural data to be acquired quickly.

Acknowledgements

The authors are grateful to Patricia Stone Wilkinson and Christiane Grzonka at Bruker Instruments Inc. for performing the LC–NMR analysis of the glyburide in vitro sample.

References

[1] R.E. Marsh and R.J. Hughes (Editors), Quadrupole Storage Mass Spectrometry, Wiley, New York, 1989.
[2] R.E. Marsh and J.F.J. Todd (Editors), Practical Aspects of Ion Trap Mass Spectrometry, CRC Press, Boca Raton, FL, 1995.
[3] C. Dollery (Editor), Therapeutic Drugs, Churchill Livingstone, New York, NY, 1991, pp. G21–G26.
[4] D.G. Kaiser and A.A. Forist, in H. Rifkin et al. (Editors), Micronase: Pharmacological and Clinical Evaluation, Excerpta Medica Foundation International Congress Series No. 382, Princeton, NJ, 1975, pp. 31–41W.
[5] W. Heptner, H.M. Kellner, O. Christ, D. Weihrauch, Arzneimittel-Forschung 19(Suppl.) (1969) 1400–1404.
[6] W. Rupp, O. Christ, W. Fulberth, Arzneimittel-Forschung 19(Suppl.) (1969) 1428–1434.
[7] S.E. Clarke, A.D. Ayrton, R.J. Chenery, Xenobiotica 24 (1994) 517–526.
[8] A. Colorado and J.S. Brodbelt, Proceedings of the 41st ASMS Conference on Mass Spectrometry and Allied Topics, San Francisco, 1993, pp. 860a–860b.
[9] L.C.E. Taylor, R. Singh, S.Y. Chang, R.L. Johnson, J. Schwartz, Rapid Commun. Mass Spectrom. 9 (1995) 902–910.
[10] K. Otsubo, S. Morita, M. Uchida, Bioorg. Med. Chem. Lett. 3 (1993) 1633–1636.
[11] K. Otsubo, J. Matsubara, T. Ohtani, Y. Kawano, K. Kitano, S. Morita, K. Kondo, Y. Yamamura, M. Uchida, Heterocycles 43 (1996) 2627–2642.
[12] J. Schwartz, J.P.E. Syka, I. Jardine, J. Am. Soc. Mass Spectrom. 2 (1991) 198–204.
[13] J.L. Josephs, M.J. Sweeney, D.C. Gale and M. Sanders, Proceedings of the 44th ASMS Conference on Mass Spectrometry and Allied Topics, Portland, 1996, p. 600.
[14] J.L. Josephs, Proceedings of the 44th ASMS Conference on Mass Spectrometry and Allied Topics, Portland, 1996, p. 974.
[15] L. Lopez, A. Land and V. Sekhar, Proceedings of the 45th ASMS Conference on Mass Spectrometry and Allied Topics, Palm Springs, 1997, in press.
[16] P.R. Tiller, Z. El Fallah, V. Wilson, J. Huysman and D. Patel, Rapid Commun. Mass Spectrom., (1997) in press.